

黔东南三穗下寒武统黑色岩系中 钒富集机制研究

www.
geojournals.cn/georev薛忠喜^{1, 2)}, 高军波^{1, 2)}, 杨瑞东^{1, 2)}, 徐海^{1, 2)}, 陈军^{1, 2)}, 高磊^{1, 2)}

1) 贵州大学资源与环境工程学院, 贵阳, 550025;

2) 贵州大学喀斯特地质资源与环境教育部重点实验室, 贵阳, 550025

内容提要: 扬子板块南缘下寒武统黑色页岩地层中分布有一套富含 Ni、Mo、V、U、Ba、PGE 等的多金属层, 并在贵州多地形成 Ni—Mo—V—Ba 矿床。黔东南三穗钒矿是扬子板块南缘黑色页岩型多金属矿床的重要组成部分, 矿体主要赋存于早寒武世九门冲组底部黑色炭质、硅质泥岩中。针对三穗钒矿含矿岩系, 通过沉积学和元素地球化学研究, 结果表明, 赋矿硅质岩、含钒炭质泥岩中存在热水物质贡献的明显信号, 指示热水端元输入很可能是钒的重要来源。环境敏感元素及相关参数分析显示, 局限盆地内的缺氧水体环境更有利于钒的富集。此外, 有机质与钒富集之间具有明显的耦合关系, 说明有机质的吸附对钒的沉淀和富集起到重要控制作用。

关键词: 下寒武统; 钒矿床; 沉积环境; 矿床成因; 黔东南

埃迪卡拉纪(震旦纪)—寒武纪(E—C)转换时期是古海洋环境演变、古生产力变革、生命演化和多金属成矿的关键时期(向雷等, 2015; 赵相宽等, 2018)。这一时期, 华南下寒武统黑色岩系中普遍发育一套富集 Ni、Mo、V、PGE、Ba 等的多金属的硫化物层(范德廉等, 1973; Fan Delian et al., 1984; Coveney et al., 1991, 1992)。该多金属层厚度较小, 通常为几厘米到十几厘米, 但横向展布范围广且较为连续(Mao Jingwen et al., 2002; Xu Lingang et al., 2021)。受古地理环境、构造活动、生物有机质等因素综合制约, Ni、Mo、V、PGE、Ba 等元素具有明显的空间分异和差异性富集特征, 其中在贵州境内表现尤为明显(Murowchick et al., 1994; Mao Jingwen et al., 2002; 魏怀瑞等, 2017)。

作为探索寒武纪生命演化、复杂环境下多金属元素超常富集的重要窗口, 早寒武世多金属层长期备受关注。通过长期深入地探索与研究, 围绕该多金属层的物质来源、富集机理、控制要素等取得了大量卓有成效的成果和认识(范德廉等, 1973; 毛景文等, 2001; Mao Jingwen et al., 2002; 杨瑞东等, 2005, 2007; Orberger et al., 2007; 温汉捷等,

2010; Han Tao et al., 2015; Fan Haifeng et al., 2020; Lu Zhitong et al., 2021)。但相比而言, 以往研究更多地工作集中在 Mo、Ni 多金属层方面, 对此提出了不同的理论认识。目前主流的观点有两种: 一种支持海水成因说, 认为成矿物质从海水中直接沉淀成矿(Mao Jingwen et al., 2002; Lehmann et al., 2007; Xu Lingang et al., 2013); 另一种观点强调热水成因说, 指出成矿物质主要来自海底热水系统(李胜荣等, 1995; Steiner et al., 2001; 杨瑞东等, 2005; Jiang Shaoyong et al., 2007; Han Tao et al., 2017)。与之对比, 对于寒武系黑色岩系型钒矿的研究相对较为薄弱(Han Tao et al., 2018; Lu Zhitong et al., 2021), 且在成矿物质来源方面存在海底热水系统(Han Tao et al. 2018)与海水来源(Xu Lingang et al. 2021)的观点分歧。此外, 海水的氧化还原条件对钒的富集有重要影响(Murowchick et al., 1994; Jiang Shaoyong et al., 2007; Lehmann et al., 2016; Han Tao et al., 2018; Pagès et al., 2018; 付勇等, 2021; Xu Lingang et al. 2021), 且早寒武世古海水环境状况及时空演化较为复杂, 目前仍是研究重点之一(温汉捷等, 2010;

注:本文为贵州省沉积矿床科技创新人才团队项目(编号:黔科合平台人才[2018]5613)、国家自然科学基金资助项目(编号:U1812402、42163006)和贵州省人才基地项目(编号:RCJD2018-21)的成果。

收稿日期:2021-04-15; 改回日期:2021-07-09; 网络首发:2021-08-20; 责任编辑:刘志强。Doi: 10.16509/j.georeview.2021.08.041

作者简介: 薛忠喜, 男, 1996 年生, 硕士研究生, 沉积矿床专业; Email: luopuxue1996@163.com。通讯作者: 高军波, 男, 1985 年生, 博士, 副教授, 硕士生导师, 主要从事沉积矿床研究和教学工作; Email: gaojunbo1985@126.com。

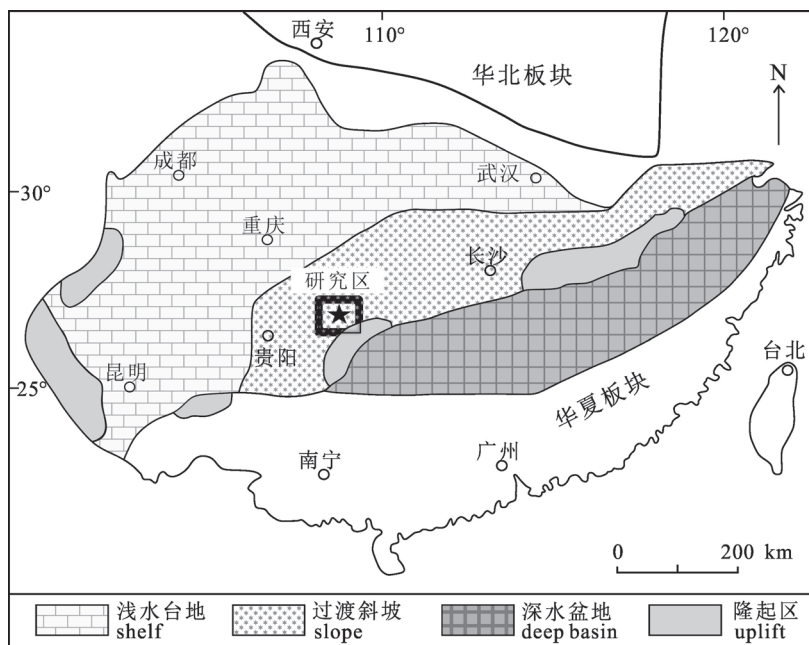


图 1 扬子地块埃迪卡拉纪晚期至早寒武纪古地理格架

(据 Chang Huajin et al. , 2018, 修改)

Fig. 1 Simplified paleogeographic map of the Yangtze Platform during the late Ediacaran to the earliest Cambrian (modified from Chang Huajin et al. , 2018)

Li Chao et al. , 2010, 2017; 向雷等, 2015; 赵相宽等, 2018)。

综上,对于钒的来源、富集过程和关键控制要素研究有待深入。解开上述科学谜题,将有助于更加深刻、全面地理解早寒武世多金属层成矿作用过程,摸清成矿规律和控矿要素。本文拟以黔东南三穗亚茶钒矿为研究对象,通过对含矿岩系沉积序列进行详细观察,并辅以系统地元素地球化学研究,探究成矿物质来源,揭示钒矿沉积时的古海水氧化还原条件,阐释钒富集与环境条件、有机质等之间的内在联系,为深刻理解华南早寒武世多金属层的成因和成矿规律提供科学依据。

1 区域与矿区地质特征

扬子地块是在约 820 Ma 由裂解大陆边缘发展而来的独立块体 (Zhao Junhong et al. , 2011; Li Chao et al. , 2017)。E—C 过渡时期,黑色岩系建造在扬子地块各相区广泛分布,层位稳定,并可进行全球对比。黑色岩系虽在扬子地块不同相区沉积特征有所差异,但整体上继承了新元古代末期的沉积格局(向雷等, 2015)。E—C 过渡时期,沿水深梯度分布的古海洋沉积物,从西北到东南可划分出 4 个不

同的相区,包括浅水台地、过渡斜坡、隆起区和深水盆地相区(图 1; Steiner et al. , 2001)。其中,浅水台地相以沉积碳酸盐岩为主,并含有一套磷质沉积;过渡斜坡相主要沉积硅质灰岩—硅质岩、泥页岩;深水盆地相以沉积层状硅质岩为主 (Goldberg et al. , 2007; 赵相宽等, 2018)。众多周知,海水的氧化还原条件对金属元素的富集有重要影响 (Jiang Shaoyong et al. , 2007; Han Tao et al. , 2018; Pagès et al. , 2018)。E—C 过渡时期,扬子地块不同相区海水的氧化还原结构较为复杂(付勇等, 2021),其中浅水台地区海水基本氧化,过渡斜坡相区以缺氧硫化为主,深水盆地相区则呈现缺氧铁化(Li Chao et al. , 2010)。另有研究认为,早寒武世海洋氧化还原环境在时空上呈现波动变化特征,指出至寒武纪第 4 阶,海洋的氧化可能才达到相对稳定状态 (Li Chao et al. , 2017)。

黔东南三穗钒矿床古地理位置处于过渡斜坡相区(图 1),矿区出露地层由老至新分别为:南华系南沱组、上震旦统陡山沱组、震旦—寒武系穿时地层留茶坡组、下寒武统九门冲组、变马冲组和杷榔组等(图 2a)。区内断裂构造较为发育,北部有一条北西向的龙田湾断层 F₁,南部有一条北西向的鸡蛋沟断层 F₂。钒矿层主要分布于留茶坡组中上部及九门冲组下部,赋矿岩石为硅质泥岩、炭质泥岩(图 2b),矿层底板为留茶坡组硅质岩,顶板为九门冲组板状炭质页岩。矿体呈层状、似层状产出,厚度沿走向及倾向变化较小,分布较为稳定。含矿岩系岩性组成由上至下依次为:

九门冲组:

未见顶

10. 灰黑色薄层炭质泥岩、硅质岩
9. 深黑色炭质泥岩,为钒富集层。厚 15~30 cm
8. 薄层状黑色硅质岩、炭质泥岩,钡含量较高,发育大量磷结核
7. 黑色纹层状炭质泥岩,为钒富集层。厚 5~10 cm

整合

留茶坡组:

6. 火山灰层,顶部硫化物含量升高
5. 深黑色薄层状带状硅质岩,夹层厚 2~3 cm 粉

末状炭质泥岩。该层顶部夹有一层 5~10 cm 厚硫化物层, 硫化物以黄铁矿为主, 表面风化呈赤红色、褐红色。
厚 1.5~2 m
4. 薄层状黑色炭质泥岩、硅质岩, 层厚 1~20 cm。位于该层底部约 1.5 m 处, 分布层厚约 20 cm 的硅质岩层间常夹薄层硫化物层。厚约 20 m
3. 灰黑色薄层状硅质岩与黑色炭质泥岩互层, 两者界限清晰, 层厚 5~20 cm。局部夹透镜状灰岩, 透镜体厚 0~80 cm, 横向延伸 2~5 m。灰岩结晶较细, 其顶底均为灰黑色致密硅质岩。
厚 3 m
陡山沱组:
2. 浅灰白色、灰绿色白云岩, 发育平行层理。
厚约 15 m
1. 条带状、纹层状硅质岩、炭质泥岩
未见底

2 样品采集和测试方法

2.1 样品采集

黔东南三穗亚茶钒矿区陡山沱组、留茶坡组、九门冲组沉积连续, 含矿岩系出露较好, 自下而上共采集样品 21 件, 其中陡山沱组 2 件, 留茶坡组 13 件, 九门冲组 6 件, 采样位置见图 2b。样品主要为硅质岩、炭质泥岩, 含钒炭质泥岩等。

2.2 测试方法

主量元素和有机碳测试在广州澳实测试中心完成。测试过程为: 先称取 50 mg 粉末样品用 250 mg 偏硼酸锂高温溶解, 随后用去离子水稀释至 100 mL 后使用电感耦合等离子体原子发射光谱仪 (ICP-AES) 仪器测试。总有机碳 (TOC) 分析采用

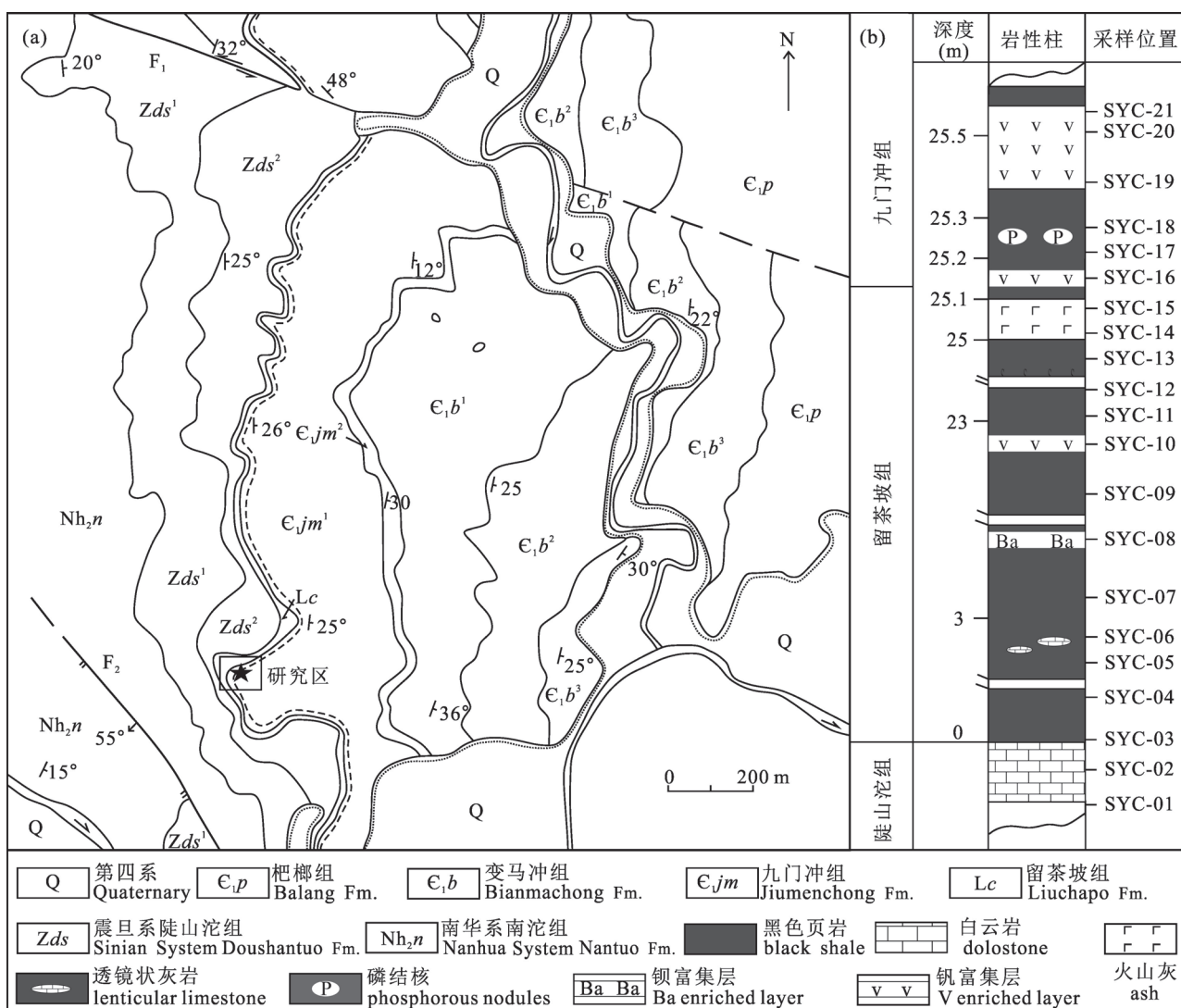


图 2 黔东南三穗钒矿区地质图及研究区地层剖面图(据邓旭升等, 2014, 修改)

Fig. 2 Geological map of the Sansui vanadium deposit in Southeastern Guizhou and stratigraphic section of the study area (modified from Deng Xusheng et al., 2014&)

表 1 黔东南三穗钒矿地球化学数据及参数特征

Table 1 Geochemical data and parameter characteristics of the Sansui vanadium deposit in Southeastern Guizhou

样 品 号	Mo	TOC (%)	Mo TOC	V	EF(V)	Ba	EF(Ba)	EF(Mo)	EF(U)	Th/U	U/Th	Y/Ho	U	Al ₂ O ₃ (%)	lg w(U) μg/g	lg w(Th) μg/g
21	43.50	7.07	6.15	2185	39.21	3597	12.56	55.68	23.04	0.21	4.80	34.64	33.6	7.91	1.53	0.85
20	34.20	8.07	4.24	2142	42.22	3561	13.66	48.09	28.93	0.16	6.32	37.55	38.4	7.20	1.58	0.78
19	89.30	14.80	6.03	7233	54.52	3404	4.99	48.01	36.01	0.04	23.90	28.97	125	18.83	2.10	0.72
18	20.10	3.52	5.71	1591	31.02	2877	10.91	27.95	26.00	0.18	5.43	37.64	34.9	7.28	1.54	0.81
17	12.78	1.44	8.88	608.8	176.3	3421	192.8	264.1	115.3	0.05	20.59	46.14	10.42	0.49	1.02	-0.30
16	43.00	7.06	6.09	7827	79.81	5833	11.57	31.28	17.53	0.39	2.57	34.88	45.0	13.92	1.65	1.24
15	20.10	1.10	18.27	1771	12.99	11404	16.27	10.52	6.03	0.82	1.21	29.37	21.5	19.35	1.33	1.25
14	22.10	1.18	18.73	1973	14.58	7825	11.25	11.65	5.65	0.82	1.22	29.87	20.0	19.21	1.30	1.21
13	28.60	3.64	7.86	1355	437.2	2404	150.8	658.1	218.2	0.03	30.20	39.25	17.7	0.44	1.25	-0.23
12	16.54	2.16	7.66	776.4	290.0	1326	96.38	440.7	132.7	0.06	18.09	39.15	9.3	0.38	0.97	-0.29
11	10.30	2.47	4.17	843.0	166.2	1860	71.33	144.8	72.47	0.07	14.27	49.25	9.62	0.72	0.98	-0.17
10	19.70	3.25	6.06	2970	240.9	6623	104.5	114.0	80.27	0.09	10.61	37.76	25.9	1.75	1.41	0.39
09	5.17	0.60	8.62	423.0	166.8	7474	573.3	145.4	118.0	0.07	13.98	47.93	7.83	0.36	0.89	-0.25
08	8.65	1.54	5.62	1114	287.5	82106	4122	159.2	80.96	0.06	15.97	40.83	8.21	0.55	0.91	-0.29
07	2.86	2.81	1.02	64.70	3.18	196.0	1.87	10.02	7.62	0.93	1.08	28.66	4.06	2.89	0.61	0.58
06	0.46	0.48	0.96	19.70	1.65	111.0	1.81	2.76	4.08	1.65	0.61	32.79	1.27	1.69	0.10	0.32
05	0.41	0.08	5.06	20.40	1.39	139.0	1.85	1.97	1.40	4.44	0.23	30.72	0.538	2.08	-0.03	0.38
04	0.83	0.64	1.30	25.80	0.90	437.0	2.95	2.05	1.18	4.16	0.24	27.26	0.888	4.09	-0.05	0.57
03	3.99	1.33	3.00	56.30	4.44	5061	77.64	22.44	2.83	1.59	0.63	29.26	0.938	1.80	-0.03	0.17

注:表中样品号前省去了“SYC-”;微量元素含量单位为:μg/g。

LecoCS230 碳硫分析仪, 相对标准偏差优于 5%。

微量元素测试在中国科学院地球化学研究所矿床地球化学国家重点实验室完成。测试过程为:称取 50 mg 于聚四氟乙烯坩埚中, 加入 1 mL 氢氟酸和 1 mL 氢硝酸; 将上述坩埚放入钢套中密封, 置于烘箱于 185°C 加热 35 h 消解样品; 待冷却后取出坩埚, 置于低温电热板上蒸干, 加入 1 mL 氢硝酸继续蒸干完全。最后于坩埚中加入 200 ng 的 Rh 内标溶液, 2 mL 氢硝酸, 3 mL 去离子水, 重新置于钢套中, 于 140°C 加热 5 h。冷却后取出坩埚, 摆匀, 取 0.4 mL 溶液至离心管中, 定容至 10 mL, 最后在 ICP-MS 上测定。测试结果列于表 1。

3 结果

3.1 有机碳(TOC)含量特征

SYC 剖面自下而上, TOC 总体处于逐渐升高的趋势。其中, 留茶坡组 TOC 含量变化介于 0.08%~3.64%。火山灰层附近, TOC 值为 1.1% 左右。与留茶坡组相比, 九门冲组 TOC 含量整体较高, 特别是钒富集层 TOC 含量最高, 可达 14.80% (SYC-19, V=7233 μg/g)。

3.2 元素地球化学特征

为了有效评估部分重要微量元素在黑色岩系中的富集程度, 特采用如下公式进行元素富集系数计

算, 公式为 (Tribouillard et al., 2006, 2012):

$$EF(X) = \frac{\frac{w(X)}{w(Al)}_{\text{样品}}}{\frac{w(X)}{w(Al)}_{\text{AUC}}}$$

式中 X 是指所采用指示元素 (如 Mo、U), AUC 指平均上地壳值 (McLennan, 2001)。计算结果表明, Mo、U、V 富集程度在留茶坡组表现为逐渐升高的趋势, 在火山灰层则显著降低。九门冲组钒富集层处具有一次明显的升高, 之后逐渐降低。相对而言, Th/U 值则呈现出相反的变化规律。Mo/TOC 值除火山灰层附近大于 15 外, 其余层位均小于 15。U/Th 值在留茶坡组逐渐升高, 至火山灰层明显下降。九门冲组钒、钡富集层处 U/Th 值再次表现高值。Y/Ho 值为 27.26~49.25, 平均 35.89。

4 讨论

4.1 沉积环境分析

钼是一种氧化还原敏感元素, 在有机物参与下, 容易在硫化水体中富集 (Tribouillard et al., 2004, 常华进等, 2009)。在没有外界条件干扰时, 海水沉积物中的 Mo 能够有效约束古海洋硫化状态, 当 Mo 浓度依次为 >100 μg/g、25~100 μg/g、<25 μg/g 时, 分别指示古海洋环境为持续性硫化、间歇性硫化、无

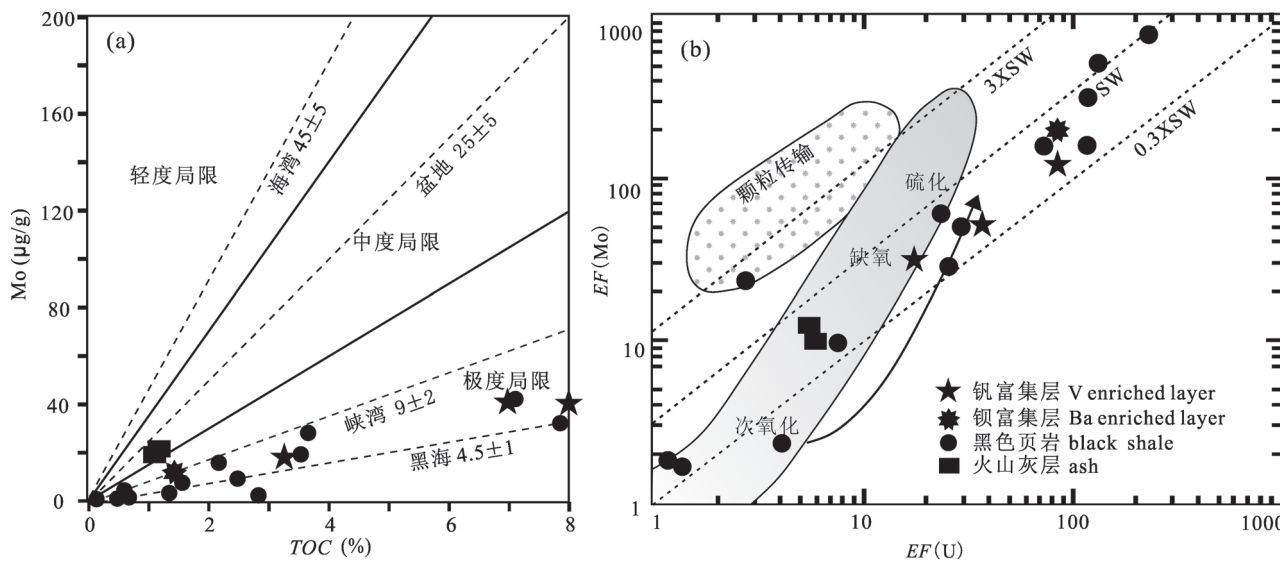


图3 黔东南三穗钒矿沉积环境判别图解(据 Algeo et al., 2006 修改)

Fig. 3 Discrimination diagram of sedimentary environment of the Sansui vanadium deposit in Southeastern Guizhou
(modified from Algeo et al., 2006)

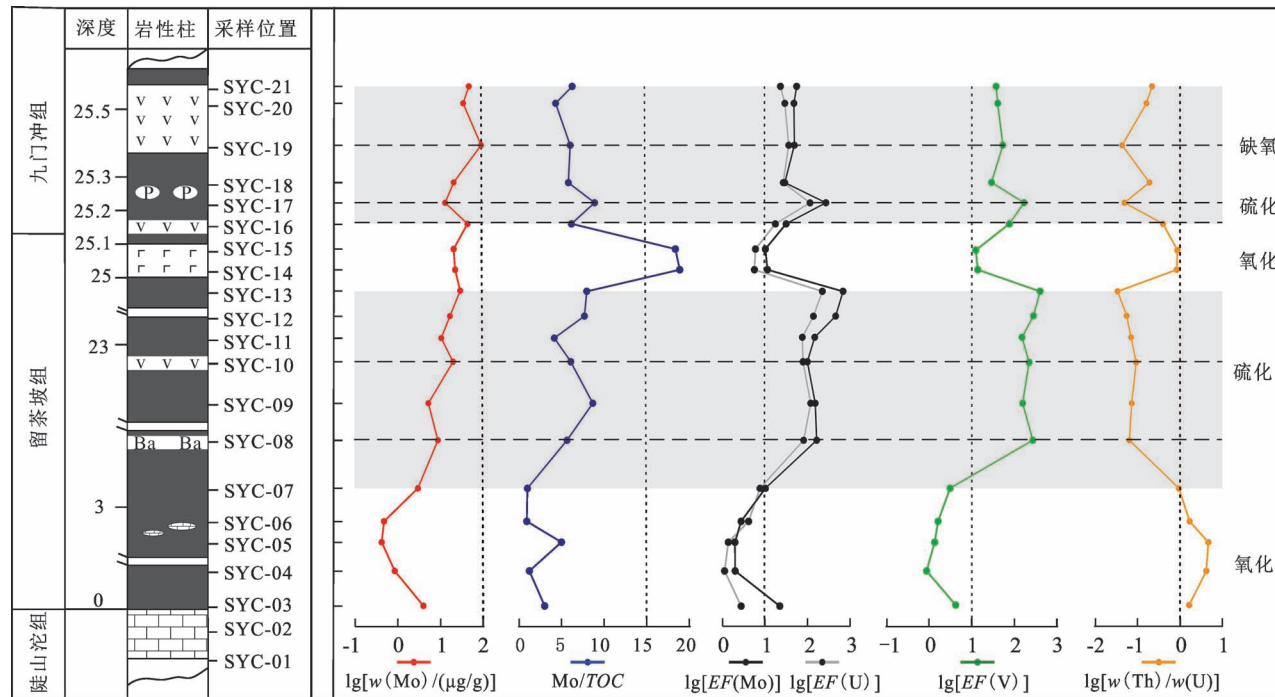


图4 黔东南三穗钒矿 Mo、Mo/TOC、EF(Mo)、EF(U)、EF(V)、Th/U 纵向变化规律

Fig. 4 The vertical variation of Mo, Mo/TOC, EF(Mo), EF(U), EF(V), Th/U in the Sansui vanadium deposit, Southeastern Guizhou

硫化状态(Scott et al., 2008)。但是,当受风化输入减弱、硫化水体面积增大等因素影响,Mo浓度会在短时间内降低到上地壳平均水平(Scott et al., 2008; Algeo et al., 2012)。另有研究指出,沉积盆地内缺氧—硫化水体Mo/TOC值与海水中Mo浓度

呈正相关关系,但沉积盆地的局限程度对Mo有一定影响,若盆地受限较强,海水中的Mo同样会亏损严重(Algeo et al., 2006, 2012)。故此,根据Mo/TOC值可间接判别盆地局限程度,其中Mo/TOC值为>35、15~35和<15分别反映轻度、中度和极度局

限盆地环境(Algeo et al., 2012)。

SYC 剖面留茶坡组和九门冲组黑色岩系的 Mo/TOC 值显示,其沉积时所处环境为极度局限环境(图 3a)。EF(Mo)与 EF(U)相关性分析表明,大多数样品均在现代海水的 0.3 倍和 1 倍之间(图 3b),也反映黑色岩系沉积时受开放海洋补给有限(Algeo et al., 2012)。E—C 过渡时期,黔东南三穗亚茶一带位于过渡斜坡相区(图 1),虽然寒武纪早期发生的海侵事件会促使过渡斜坡相区与开放海洋的连通性增强(Li Chao et al., 2017),但仍有部分地区与开放海洋相隔(Goldberg et al., 2007)。

一般来讲,沉积水体中 Th/U 值介于 0~2.0 代表缺氧环境,2.0~8.0 代表次氧化—氧化环境,大于 8.0 为氧化环境(Kimura et al., 2001; Chang Huajin et al., 2012)。另外,EF(Mo)、EF(U)、EF(V)富集系数,以及 EF(Mo)—EF(U)协变图解也可用于判断沉积水体的氧化还原条件(Tribouillard et al., 2012; 向雷等, 2015)。上述环境敏感元素及比值综合研究表明,SYC 剖面留茶坡组下部环境为氧化条件,中部沉积环境由氧化条件转为硫化状态,靠近顶部硫化程度则进一步加强。在火山灰层附近,沉积环境发生了一次明显的动荡,存在硫化—氧化(氧化)—硫化的骤变过程。在九门冲组底部,沉积

环境由硫化转化为缺氧条件,且缺氧程度相比留茶坡组有所减弱(图 3 和图 4)。通过分析钒富集与环境演变之间的关系可以发现,SYC 剖面中钒富集往往处于盆地极度局限,且水体为缺氧状态的海水环境中。这种环境往往有利于钒的富集甚至成矿(Han Tao et al., 2018)。

4.2 钒富集机制探讨

已有研究表明,扬子地块在寒武纪早期存在广泛的热液活动(Han Tao et al., 2017)。热水沉积岩的 U/Th>1,正常沉积岩的 U/Th<1(Rona, 1978)。SYC 剖面 U/Th 值在留茶坡组中上部显著偏正,特别是钒富集层(SYC-08)处显著升高。同时,在九门冲组钒富集层附近,U/Th 值也明显升高(图 5),表明可能存在多幕式的热水活动特点。在火山灰层附近 U/Th 值相对降低,反映了热水活动间歇期沉积的特征。

海水的 Y/Ho 值一般为 44~74,而球粒陨石、火山岩和页岩的比值为 26~28(Nozaki, 1997)。黔东南三穗亚茶样品的 Y/Ho 值(27.26~49.25,平均 35.89)明显低于海水,但接近球粒陨石、火山岩和页岩(Nozaki, 1997)。同时,考虑到三穗地区受火山活动的影响,可能导致 Y/Ho 值较低。因此,综合其他指标(U/Th 等),含 V 炭质泥岩较低的 Y/Ho

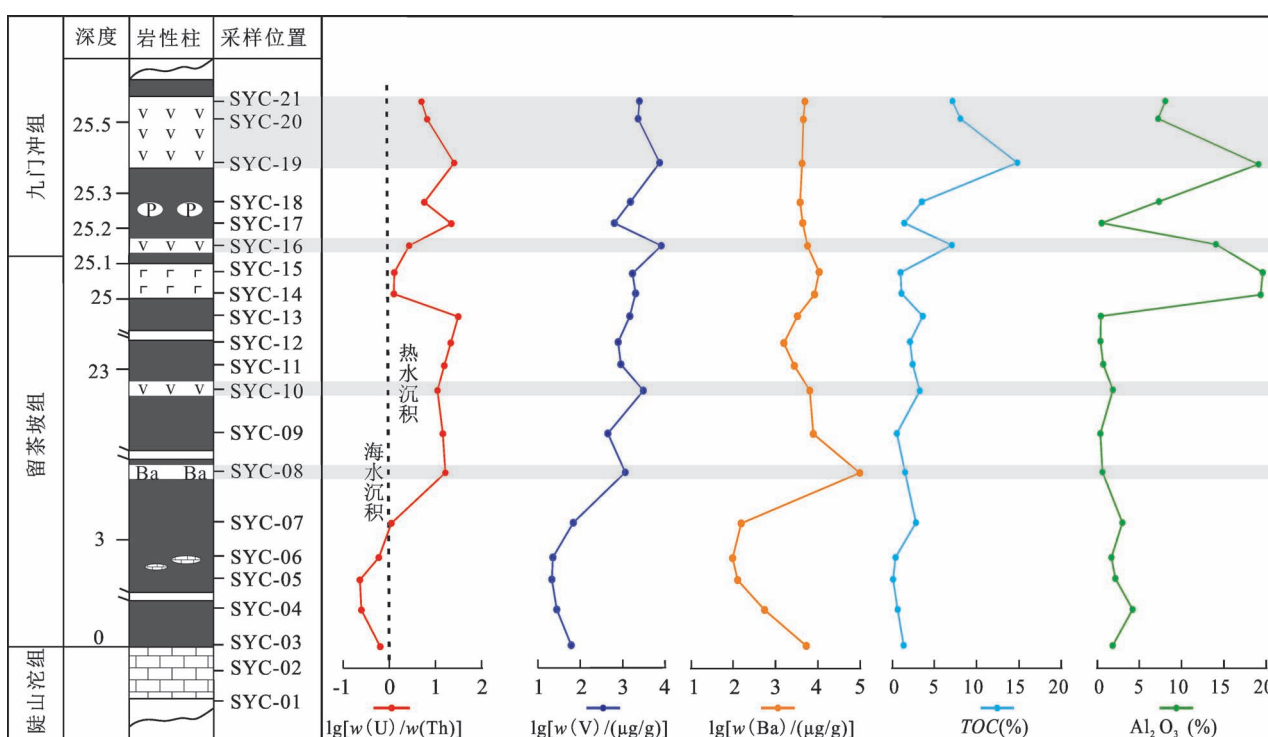


图 5 黔东南三穗钒矿 U/Th、V、Ba、TOC、 Al_2O_3 纵向变化规律

Fig. 5 The vertical variation of U/Th, V, Ba, TOC and Al_2O_3 in the Sansui vanadium deposit, Southeastern Guizhou

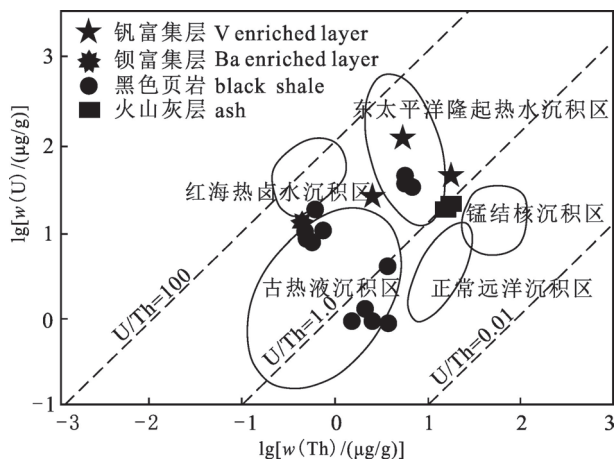


图6 黔东南三穗钒矿 U—Th 含量双对数图解
(据 Boström, 1983 修改)

Fig. 6 U—Th bilogarithmic diagram of Sansui vanadium deposit in Southeastern Guizhou (modified from Boström, 1983)

值实质反映了热液物质的积极参与。

三穗钒矿中火山灰层的存在,表明区内曾存在火山活动。通过对三穗钒矿含矿岩系 $\lg U - \lg Th$ 关系进行分析,发现留茶坡组硅质岩、含钒页岩主要落在古热液沉积区和太平洋隆起沉积区(图6),火山灰层中 V 含量也达到 $1771 \sim 1973 \mu\text{g/g}$,说明热水端元输入很可能是钒的主要来源之一。

与留茶坡组相比,九门冲组 Al_2O_3 含量整体偏高,除 SYC-17 ($\text{Al}_2\text{O}_3 = 0.49\%$) 外,介于 $7.20\% \sim 18.83\%$ 。通过对比分析含钒炭质、硅质泥岩中

Al_2O_3 含量特征及变化规律发现,样品中钒含量较高时,往往伴随 Al_2O_3 含量的偏高。譬如,样品 SYC-16 和 SYC-19 的 V 含量很高,分别为 $7827 \mu\text{g/g}$ 和 $7233 \mu\text{g/g}$,对应 Al_2O_3 含量分别达到 13.92% 、 18.83% ,这些特征表明,强烈的大陆风化诱导的陆源物质输入很可能为钒的富集成矿提供物质供应。另外,海洋系统 Mo 库大小除受硫化水体面积影响外,大陆风化物质输入也是重要影响因素之一(Scott et al., 2008),特别是当陆源风化物质输入占据主导时,沉积物往往含有较高 Mo 含量。SYC-19 不仅具有较高的 V、 Al_2O_3 含量,Mo 含量也达到 $89.3 \mu\text{g/g}$,这进一步印证了大陆风化输入的可能性。

研究表明,钒常以类质同象的形式存在于水云母中,部分以吸附状态赋存于炭质页岩中,或以游离氧化物形式存在(陈建华等, 2007; 朱红周等, 2010)。三穗钒矿主要赋矿岩石为炭质泥岩或页岩,扫描电镜观察发现钒多以吸附状态赋存在伊利石等黏土矿物中(图7)。近年来研究表明,有机质吸附是引起钒富集的重要环节(Han Tao et al., 2018),成岩阶段经有机质降解,钒被释放后与黏土矿物结合,形成以含钒伊利石为主要载体的钒矿床(Lu Zhitong et al., 2021)。本文通过对三穗钒矿黑色岩系中 V 和 TOC 协变关系研究也发现,两者具有相似的变化规律(图5),当钒显著富集时,TOC 含量则明显偏高,反之则明显降低,说明缺氧的还原环境有利于 TOC 的富集(夏鹏等, 2020),TOC 对钒的富集起到重要固定作用。

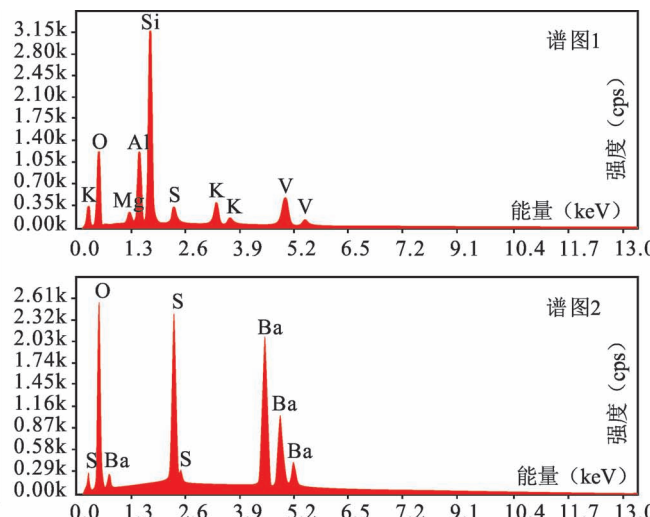
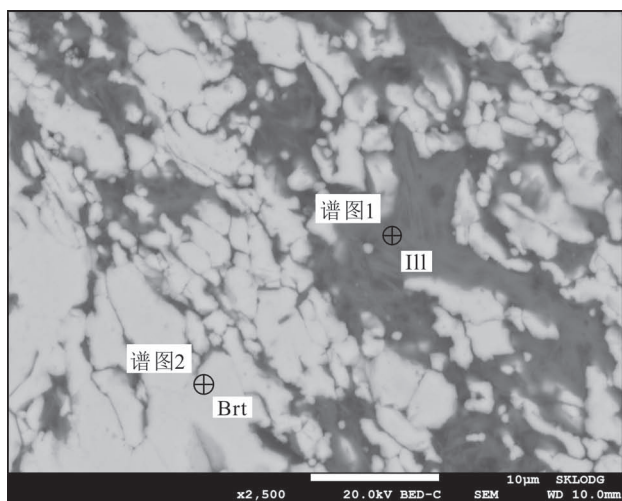


图7 黔东南三穗钒矿扫描电镜与能谱分析图

Fig. 7 SEM and EDS analysis of the Sansui vanadium deposit in Southeastern Guizhou

综上,热水系统诱导的深部物质循环和大陆风化促使的陆源碎屑物质输入,奠定了钒富集成矿所需的物质基础。而局限盆地内的缺氧水体环境为钒成矿创造了有利条件,加之有机质的吸附,共同促进并制约着钒的沉淀和富集成矿过程。

5 结论

黔东南三穗钒矿是扬子板块南缘早寒武世黑色岩系型多金属矿床的重要组成部分。本文通过对三穗钒矿沉积学、元素地球化学开展深入研究,取得如下主要认识:

(1)三穗钒矿含矿岩系以黑色炭质、硅质泥岩为主,赋矿地层主要为早寒武世九门冲组,次为留茶坡组。

(2)三穗钒矿成矿物质具有多来源特征,其中热水系统诱导的深部物质循环,以及强烈的大陆风化导致的陆源物质输入,很可能是钒富集成矿的重要物质基础。

(3)局限盆地内发育的缺氧环境为钒的富集成矿创造了有利条件,有机质吸附是引起钒沉淀和成矿的重要途径。

致谢:样品测试分析得到了中国科学院地球化学研究所矿床学地球化学国家重点实验室胡静和董少花老师的指导和帮助,论文撰写过程中与课题组同仁进行了大量有益探讨,在此一并感谢。

参 考 文 献 / References

(The literature whose publishing year followed by a “&” is in Chinese with English abstract; The literature whose publishing year followed by a “#” is in Chinese without English abstract)

- 常华进, 储雪蕾, 冯连君, 黄晶, 张启锐. 2009. 氧化还原敏感微量元素对古海洋沉积环境的指示意义. 地质论评, 55(1): 93~101.
- 陈建华, 彭家强, 温官国. 2007. 贵州松桃下寒武统九门冲组钼钒矿的赋存状态初步研究. 贵州地质, 24(3): 185~187.
- 邓旭升, 李明琴, 张梅江. 2014. 贵州三穗八弓钒矿床岩、矿石特征及其成因初探. 贵州大学学报, 31(3): 41~44.
- 范德廉, 杨秀珍, 王连芳, 陈南生. 1973. 某地下寒武统含镍钼多元素黑色岩系的岩石学及地球化学特点. 地球化学, (3): 143~164.
- 付勇, 周文喜, 王华建, 谢文浪, 叶云涛, 江冉, 王晓梅, 苏劲, 李迪, 夏鹏. 2021. 黔北下寒武统黑色岩系的沉积环境与地球化学响应. 地质学报, 95(2): 536~548.
- 李胜荣, 高振敏. 1995. 湘黔地区牛蹄塘组黑色岩系稀土特征——兼论海相热水沉积岩稀土模式. 矿物学报, 15(2): 225~229.
- 毛景文, 张光弟, 杜安道, 王义天, 曾明果. 2001. 遵义黄家湾镍钼族元素矿床地质、地球化学和 Re-Os 同位素年龄测定——兼论华南寒武系底部黑色页岩多金属成矿作用. 地质学报, 75(2): 234~243.

- 魏怀瑞, 杨瑞东, 高军波. 2017. 贵州寒武系底部黑色岩系热水沉积成矿过程与热水沉积矿床研究. 贵阳: 贵州科技出版社.
- 温汉捷, 张羽旭, 樊海峰, 胡瑞忠. 2010. 华南下寒武统地层的 Mo 同位素组成特征及其古海洋环境意义. 科学通报, 55(2): 176~181.
- 夏鹏, 付勇, 杨镇, 郭川, 黄金强, 黄明勇. 2020. 黔北镇远牛蹄塘组黑色页岩沉积环境与有机质富集关系. 地质学报, 94(3): 947~956.
- 向雷, 蔡春芳, 贺训云, 姜磊, 袁余洋, 汪天凯, 贾连奇. 2015. 华南李家沱剖面寒武纪纽芬兰世海水氧化还原性质演化及其驱动因素. 地球科学(中国地质大学学报), 40(7): 1197~1214.
- 杨瑞东, 朱立军, 高慧, 张位华, 姜立君, 王强, 鲍森. 2005. 贵州遵义松林寒武系底部热液喷口及与喷口相关生物群特征. 地质论评, 51(5): 481~492.
- 杨瑞东, 魏怀瑞, 鲍森, 王伟, 王强. 2007. 贵州天柱上公塘—大河边寒武纪重晶石矿床海底热水喷流沉积结构、构造特征. 地质论评, 53(5): 675~680.
- 赵相宽, 史晓颖, 王新强, 汤冬杰. 2018. 寒武纪早期海洋阶段性氧化驱动早期后生动物多样化进程. 地球科学, 43(11): 73~90.
- 朱红周, 侯俊富, 原连肖, 王淑利. 2010. 南秦岭千家坪钒矿床钒赋存状态研究. 地质与勘探, 46(4): 643~648.
- Algeo T J, Lyons T W. 2006. Mo-total organic carbon covariation in modern anoxic marine environments: Implications for analysis of paleoredox and paleohydrographic conditions. Paleoceanography, 21(1): 279~298.
- Algeo T J, Rowe H. 2012. Paleoceanographic applications of trace-metal concentration data. Chemical Geology, 324~325: 6~18.
- Boström K. 1983. Genesis of ferromanganese deposits—Diagnositc criteria for recent and old deposits. In: Rona P A, Boström K, Laubier L (Eds.). Hydrothermal Processes at Seafloor Spreading Centers. Plenum Press, New York: 473~489.
- Chang Huajin, Chu Xuelei, Feng Lianjun, Huang Jing, Zhang Qirui. 2009&. Redox sensitive trace elements as paleoenvironments proxies. Geological Review, 55(1): 93~101.
- Chang Huajin, Chu Xuelei, Feng Lianjun, Huang Jing. 2012. Progressive oxidation of anoxic and ferruginous deep-water during deposition of the terminal Ediacaran Laobao Formation in South China. Palaeogeography, Palaeoclimatology, Palaeoecology, 321~322: 80~87.
- Chang Huajin, Chu Xuelei, Feng Lianjun, Huang Jing, Chen Yali. 2018. Marine redox stratification on the earliest Cambrian (ca. 542~529 Ma) Yangtze Platform. Palaeogeography, Palaeoclimatology, Palaeoecology, 504: 75~85.
- Chen Jianhua, Peng Jiaqiang, Wen Guanguo. 2007&. Preliminary study on occurrence status of molybdenum—vanadium ores of Lower Cambrian Jiumencong formation, Songtao County, Guizhou. Guizhou Geology, 24(3): 185~187.
- Coveney R M J, Chen Nansheng. 1991. Ni—Mo—PGE—Au-rich ores in Chinese black shales and speculations on possible analogues in the United States. Mineralium Deposita, 26(2): 83~88.
- Coveney R M J, Murowchick J B, Grauch R I, Michael D, Glascock D, Denison J D. 1992. Gold and platinum in shales with evidence against extraterrestrial sources of metals. Chemical Geology, 99(1~3): 101~114.
- Deng Xusheng, Li Mingqin, Zhang Meijiang. 2014&. Preparation of organic inorganic composite materials using organic impregnate geopolymers. Journal of Guizhou University, 31(3): 41~44.
- Fan Delian, Yang Xiuzhen, Wang Lianfang, Chen Nanshan. 1973&.

- Petrological and geochemical characteristics of a nickel—molybdenum—multi-element bearing lower-Cambrian black shale from a certain district in South China. *Chemical Geology*, (3): 143~164.
- Fan Delian, Yang Ruiying, Huang Zhongxiang. 1984. The Lower Cambrian black shales series and the iridium anomaly in south China: developments in geoscience. Contribution to 27th International Geological Congress, Moscow. Beijing: Science Press, 215~224.
- Fan Haifeng, Zhang Hongjie, Xiao Chaoyi, Pasava J, Han Tao, Zhou Ting, Wen Hanjie. 2020. Large Zn isotope variations in the Ni—Mo polymetallic sulfide layer in the Lower Cambrian, South China. *Gondwana Research*, 85: 224~236.
- Fu Yong, Zhou Wenxi, Wang Huijian, Qiao Wenlang, Ye Yuntao, Jiang Ran, Wang Xiaomei, Su Jin, Li Di, Xia Peng. 2021&. The relationship between environment and geochemical characteristics of black rock series of Lower Cambrian in northern Guizhou. *Acta Geologica Sinica*, 95(2): 536~548.
- Goldberg T, Strauss H, Guo Qingjun, Liu Congqiang. 2007. Reconstructing marine redox conditions for the Early Cambrian Yangtze Platform: Evidence from biogenic sulphur and organic carbon isotopes. *Palaeogeography, Palaeoclimatology, Palaeoecology*, 254(1~2): 175~193.
- Han Tao, Zhu Xiaoqing, Li Kun, Jiang Lei, Zhao Chenghai, Wang Zhonggang. 2015. Metal sources for the polymetallic Ni—Mo—PGE mineralization in the black shales of the Lower Cambrian Niutitang Formation, South China. *Ore Geology Review*, 67: 158~169.
- Han Tao, Fan Haifeng, Zhu Xiaoqing, Wen Hanjie, Zhao Chenghai, Xiao Fang. 2017. Submarine hydrothermal contribution for the extreme element accumulation during the early Cambrian, South China. *Ore Geology Reviews*, 86: 297~308.
- Han Tao, Fan Haifeng, Wen Hanjie. 2018. Dwindling vanadium in seawater during the early Cambrian, South China. *Chemical Geology*, 492: 20~29.
- Jiang Shaoyong, Yang Jinghong, Ling Hongfei, Chen Yongquan, Feng Hongzhen, Zhao Kiudong, Ni Pei. 2007. Extreme enrichment of polymetallic Ni—Mo—PGE—Au in Lower Cambrian black shales of South China: An Os isotope and PGE geochemical investigation. *Palaeogeography, Palaeoclimatology, Palaeoecology*, 254(1~2): 217~228.
- Kimura H, Watanabe Y. 2001. Oceanic anoxia at the Precambrian—Cambrian boundary. *Geology*, 29(11): 995~998.
- Lehmann B, N gler T F, Holland H D, Wille M, Mao Jingwen, Pan Jiayong, Ma Dongsheng, Dulski P. 2007. Highly metalliferous carbonaceous shale and Early Cambrian seawater. *Geology*, 35(5): 403~406.
- Lehmann B, Frei R, Xu Lingang, Mao Jingwen. 2016. Early Cambrian black shale-hosted Mo—Ni and V mineralization on the rifted margin of the Yangtze platform, China: reconnaissance chromium isotope data and a refined metallogenetic model. *Economic Geology*, 111: 89~103.
- Li Chao, Love G D, Lyons T W, Fike D A, Sessions A L, Chu Xuelei. 2010. A stratified redox model for the Ediacaran ocean. *Science*, 328: 80~83.
- Li Chao, Jin Chengsheng, Planavsky N J, Algeo T J, Cheng Meng, Yang Xinglian, Zhao Yuanlong, Xie Shucheng. 2017. Coupled oceanic oxygenation and metazoan diversification during the Early—Middle Cambrian? *Geology*, 45(8): 743~746.
- Li Shengrong, Gao Zhenmin. 1995&. REE characteristics of black rock series of niutitang formation in Hunan—Guizhou area with discussion on REE model of marine hydrothermal sedimentation. *Acta Mineralogica Sinica*, 15(2): 225~229.
- Lu Zhitong, Hu Ruizhong, Han Tao, Wen Hanjie, Algeo T J. 2021. Control of V accumulation in organic-rich shales by clay—organic nanocomposites. *Chemical Geology*, 567: 120100.
- Mao Jingwen, Zhang Guangdi, Du andao, Wang Yitian, Zeng Mingguo. 2001&. Geology, geochemistry, and Re-Os isotopic dating of the Huangjiawan Ni—Mo—PGE deposit, Zunyi, Guizhou Province—with a discussion of the polymetallic mineralization of basal Cambrian black shales in South China. *Acta Geologica Sinica*, 75(2): 234~243.
- Mao Jingwen, Zhang Guangdi, Du andao, Wang Yitian, Zeng Mingguo. 2002. Re-Os dating of polymetallic Ni—Mo—PGE—Au mineralization in Lower Cambrian black shales of South China and its geologic significance. *Economic Geology*, 97(5): 1051~1061.
- McLennan S M. 2001. Relationship between the trace element composition of sedimentary rocks and upper continental crust. *Geochemistry Geophysics Geosystems*, 2(4): 203~236.
- Murowchick J B, Coveney B M J, Grauch R I, Eldridge C S, Shelton K L. 1994. Cyclic variations of sulfur isotopes in Cambrian stratabound Ni—Mo—(PGE—Au) ores of southern China. *Geochimica et Cosmochimica Acta*, 58(7): 1813~1823.
- Nozaki Y. 1997. The fractionation between Y and Ho in the marine environment. *Earth and Planetary Science Letters*, 148(1): 329~340.
- Orberger B, Vymazalova A, Wagner C, Fialin M, Gallien J P, Wirth R, Pasava J, Montagnac G. 2007. Biogenic origin of intergrown Mo-sulphide and carbonaceous matter in Lower Cambrian black shales (Zunyi Formation, southern China). *Chemical Geology*, 238(3~4): 213~231.
- Pages A, Barnes S, Schmid S, Raymond M, Coveney J, Schwark L. 2018. Geochemical investigation of the lower Cambrian mineralised black shales of South China and the late Devonian Nick deposit, Canada. *Ore Geology Reviews*, 94: 396~413.
- Rona P A. 1978. Criteria for recognition of seafloor hydrothermal mineral deposits. *Economic Geology*, 73(2): 135~160.
- Scott C, Lyons T W, Bekker A, Bekker A, Shen Y, Poulton S W, Chu Xuelei, Anbar A D. 2008. Tracing the stepwise oxygenation of the Proterozoic ocean. *Nature*, 452: 456~459.
- Steiner M, Wallis E, Erdtmann B D, Zhao Yuanlong, Yang Ruidong. 2001. Submarine-hydrothermal exhalative ore layers in black shales from South China and associated fossils—insights into a Lower Cambrian facies and bio-evolution. *Palaeogeography, Palaeoclimatology, Palaeoecology*, 169(3~4): 165~191.
- Tribouillard N, Riboulleau A, Lyons T, Baudin F. 2004. Enhanced trapping of molybdenum by sulfurized marine organic matter of marine origin in Mesozoic limestones and shales. *Chemical Geology*, 213(4): 385~401.
- Tribouillard N, Algeo T J, Lyons T, Riboulleau A. 2006. Trace metals as paleoredox and paleoproductivity proxies: An update. *Chemical Geology*, 232(1~2): 12~32.
- Tribouillard N, Algeo T J, Baudin F, Riboulleau A. 2012. Analysis of marine environmental conditions based on molybdenum—uranium covariation—Applications to Mesozoic paleoceanography. *Chemical Geology*, 324~325: 46~58.
- Wei Huairui, Yang Ruidong, Gao Junbo. 2017#. Research on

- Hydrothermal Sedimentary Mineralization Process and Hydrothermal Sedimentary Deposits of Black Rock Series at the Bottom of Cambrian in Guizhou. Guiyang: Guizhou Science and Technology Press.
- Wen Hanjie, Zhang yuxu, Fan Haifeng, Hu Ruizhong. 2010#. Mo isotopes in the Lower Cambrian formation of southern China and its implications on paleo-ocean environment. Chinese Science Bulletin, 55(2): 176~181.
- Xia Peng, Fu Yong, Yang Zhen, Guo Chuan, Huang Jin Qiang, Huang Mingyong. 2020&. The relationship between sedimentary environment and organic matter accumulation in the Niutitang black shale in Zhenyuan, northern Guizhou. Acta Geologica Sinica, 94 (3): 947~956.
- Xiang Lei, Cai Chunfang, He Xunyun, Jiang Lei, Yuan Yuyang, Wang Tianshui, Jia Lianqi. 2015&. The ocean redox state evolution and its controls during the Cambrian Series 1~2: Evidence from Lijiatuo section, South China. Earth Science—Journal of China University of Geosciences, 40(7): 1197~1214.
- Xu Lingang, Lehmann B, Mao Jingwen. 2013. Seawater contribution to polymetallic Ni—Mo—PGE—Au mineralization in early Cambrian black shales of South China: Evidence from Mo isotope, PGE, trace element, and REE geochemistry. Ore Geology Reviews, 52: 66~84.
- Xu Lingang, Mao Jingwen. 2021. Trace element and C—S—Fe geochemistry of Early Cambrian black shales and associated polymetallic Ni—Mo sulfide and vanadium mineralization, South China: Implications for paleoceanic redox variation. Ore Geology Reviews, 135: 104210.
- Yang Ruidong, Zhu Lijun, Gao Hui, Zhang Weihua, Jiang Lijun, Wang Qiang, Bao Miao. 2005&. A study on characteristics of the hydrothermal vent and relating biota at the Cambrian bottom in Songlin, Zunyi County, Guizhou Province. Geological Review, 51 (5): 481~492.
- Yang Ruidong, Wei Huairui, Bao Miao, Wang Wei, Wang Qiang. 2007&. Submarine hydrothermal venting—flowing sedimentary characters of the Cambrian Shanggongtang and Dahebian barite deposits, Tianzhu County, Guizhou Province. Geological Review, 53(5): 675~680.
- Zhao Junhong, Zhou Meifu, Yan Danpoing, Zheng Jianping, Li Jianwei. 2011. Reappraisal of the ages of Neoproterozoic strata in South China: No connection with the Grenvillian orogeny. Geology, 39 (4): 299~302.
- Zhao Xiangkuan, Shi Xiaoying, Wang Xinjiang, Tang Dongjie. 2018&. Stepwise oxygenation of early Cambrian ocean controls early metazoan diversification. Earth Science, 43(11): 73~90.
- Zhu Hongzhou, Hou Junfu, Yuan Lianxiao, Wang Shuli. 2010&. Study on occurrence of vanadium in the Qianjiaping vanadium deposit of South Qinling. Geology and Exploration, 46(4): 643~648.

Enrichment mechanism of vanadium in Lower Cambrian black rock series in Sansui, southeastern Guizhou

XUE Zhongxi^{1, 2)}, GAO Junbo^{1, 2)}, YANG Ruidong^{1, 2)}, XU Hai^{1, 2)}, CHEN Jun^{1, 2)}, GAO Lei^{1, 2)}

1) College of Resource and Environment Engineering, Guizhou University, Guiyang, 550025;

2) Key Laboratory of Karst Georesources and Environment, Ministry of Education, Guizhou University, Guiyang, 550025

Objectives: This paper takes the Sansui Yacha section in Southeastern Guizhou, which is located in the transitional slope area of the Yangtze Block during the Ediacaran (Sinian) Period—Cambrian Period transitional time as the research object, explores the source of ore-forming materials, reveals the redox conditions of ancient seawater during the deposition of the vanadium deposits, and explains the internal relationship between vanadium enrichment and environmental conditions, organic matter. The purpose is to provide a scientific basis for a further understanding of the genesis and metallogenetic regularity of the Early Cambrian polymetallic layer in South China.

Methods: Field investigation and systematic sampling were carried out in this paper. The samples were tested for major, trace and organic carbon and further through the study of sedimentology and element geochemistry.

Results: ① From the bottom to the top of the Sansui Yacha section, TOC is gradually increasing. Compared with the Liuchapo Formation, the TOC content of the Jiumenchong Formation is higher, especially in the vanadium rich layer, which can reach 14.80%. ② The enrichment of Mo, U and V in the Liuchapo Formation increased gradually, but decreased significantly in the volcanic ash layer. In Jiumenchong Formation, there is an obvious increase at the barium enrichment layer, and then it decreases gradually. On the other hand, Th/U value shows the opposite trend. Mo/TOC values are less than 15 except for those near the volcanic ash layer. The U/Th ratio increased gradually in the Liuchapo Formation and decreased significantly in the volcanic ash layer but in the vanadium and barium enriched layer of Jiumenchong Formation is high again. Y/Ho was 27.26~49.25, with an average of 35.89.

Conclusions: ① The ore bearing rock series of the Sansui vanadium deposit is mainly composed of black

carbonaceous and siliceous mudstone. The ore bearing strata are mainly the Lower Cambrian Jiumenchong Formation, followed by the Liuchapo Formation. ② The ore-forming materials of the Sansui vanadium deposit have the characteristics of multiple sources. The deep material circulation induced by hydrothermal system and the input of terrigenous material caused by strong continental weathering are likely to be the important material basis of vanadium enrichment. ③ The anoxic environment developed in the limited basin creates favorable conditions for vanadium enrichment and mineralization, and the adsorption of organic matter is an important way to cause vanadium precipitation and mineralization.

Keywords: Lower Cambrian; vanadium deposit; sedimentary environment; genesis of deposit; southeastern Guizhou

Acknowledgements: This research is supported by Scientific and Technological Innovation Talents Team project of sedimentary deposit in Guizhou Province (No. [2018]5613), National Natural Science Fund project (Nos. U1812402, 42163006) and Guizhou talent base project (No. RCJD2018-21). Thanks all the reviewers for their constructive comments on this research

First author: XUE Zhongxi, male, born in 1996, is a master degree candidate, research direction: mineralogy, petrology, mineral deposit geology; Email: luopuxue1996@163.com

Corresponding author: GAO Junbo, male, born in 1985, associated professor, master degree candidate supervisor, is mainly engaged in the study of mineral deposit geology and geochemistry; Email: gaojunbo1985@126.com

Manuscript received on: 2021-04-15; **Accepted on:** 2021-07-09; **Network published on:** 2021-08-20

Doi: 10. 16509/j. georeview. 2021. 08. 041

Edited by: LIU Zhiqiang